Islamic Azad University

Journal of
Optoelectronical Nanostructures

Summer 2024 / Vol. 9, No. 3

Research Paper

First-Principles Study of Optical Aspects of Penta-Graphene and T-Carbon under External Stress and Hydrostatic Pressure

Hamidreza Alborznia*[,1]

[1] Department of Physics, Khatam Al-Anbia University, Tehran, Iran

Received: 12 Jul. 2024
Revised: 26 Aug. 2024
Accepted: 1 Sep. 2024
Published: 15 Sep. 2024

Keywords:
Density Functional Theory (DFT), Complex dielectric function, Absorption, reflectivity, Optoelectronic

Abstract

In this study, we present two new carbon nano allotropes: Penta-graphene and T-Carbon. Using first-principles calculations based on Density Functional Theory (DFT), we perform an extensive analysis of their crystalline structures. We delve into their optical properties, including a detailed assessment of the optical joint density of states and both the imaginary and real parts of the complex dielectric function. We also examine the reflectivity and absorption spectra to gain a full understanding of their optical characteristics. Our study takes into account special scenarios, such as the effects of hydrostatic pressure and vertical compressive stress. The shifts in optical properties we observe correlate well with the electronic characteristics of these nanostructures. Additionally, we explore the potential applications of these materials in various optoelectronic devices. Thus, we suggest their use in creating advanced optoelectronic devices, particularly as sensors designed for specific conditions, due to their unique and tunable optical properties.

10.30495/JOPN.2024.33376.1317

Citation: Hamidreza Alborznia. First-principles study of optical aspects of Penta-graphene and T-Carbon under external stress and hydrostatic pressure. **Journal of Optoelectronical Nanostructures. 2024; 9 (3): 53-76**
DOI:

***Corresponding author:** Hamidreza Alborznia
Address: Department of Physics, Khatam Al-Anbia University, Tehran, Iran.
Tell: 00989125867250 **Email:** hamidrezaalborznia@gmail.com

INTRODUCTION

Carbon, distinguished by its unique elemental properties, demonstrates an exceptional ability to form a wide array of diverse structures and nanostructures. This capability stems from its proficiency in establishing covalent bonds with both its own atoms and those of other elements, enabling the creation of complex and stable configurations. This inherent versatility leads to the formation of various carbon allotropes, such as graphene, carbon nanotubes, fullerenes, nanofibers, and other nanostructures, each with distinct characteristics and applications. These allotropes are integral to the progression of nanotechnology, offering unparalleled mechanical strength, electrical conductivity, thermal stability, and chemical reactivity. The notable physicochemical features of these carbon-based structures position them at the forefront of pioneering technological advancements, driving innovations in fields such as electronics, energy storage, biomedicine, and environmental science.

The prediction and synthesis of novel carbon structures with unique physical properties present significant potential for the advancement of innovative optoelectronic devices. The development of graphene marked a pivotal moment in this domain, catalyzing extensive research into its dynamic, electronic, and optical characteristics for the development of cutting-edge electronic and optoelectronic applications. Graphene's exceptional properties, such as its high electron mobility, mechanical strength, and optical transparency, have made it a cornerstone in the field of nanotechnology [1-12].

Building on the success of graphene, researchers have identified and predicted a diverse array of two-dimensional and three-dimensional carbon allotropes, including graphyne, graphdiyne, carbon nanoribbons, and carbon nanospheres. Each of these allotropes exhibits distinct classifications and properties, such as varying band gaps, mechanical flexibility, and thermal conductivity, which are tailored for specific applications [11-15].

The exploration of the dynamic, electronic, and optical possessions of these allotropes has become a central focus of contemporary research. This includes studying their band structure, density of states, and excitonic effects, as well as their interaction with light and other electromagnetic waves. Such investigations are crucial for understanding and optimizing their performance in devices like photodetectors, light-emitting diodes (LEDs), solar cells, and transistors [15-18].

In this article, we explore the optical aspects of two newly predicted carbon

nano allotropes Utilizing first-principles calculations grounded in Density Functional Theory. We examine their behavior under various situations, including applied pressure, mechanical deformation, and stress. Our comprehensive analysis covers the optical density of states, the imaginary and real components of the dielectric function, energy loss spectra, reflectivity, and absorption spectra. By examining these parameters, we aim to elucidate the fundamental optical characteristics of these allotropes. The insights gained from this research are pivotal for the development and optimization of innovative optoelectronic devices, providing a foundation for future technological advancements [12-14].

Computation methods

To determine the optical aspects under various conditions, we employ first-principles calculations within the basis of DFT. These computations, which eschew empirical parameters in favor of fundamental physical quantities, are crucial for accurately predicting material properties. We utilize a specialized computational code designed for both crystalline materials and nano materials, leveraging the full potential approximation. This code, founded on the linear augmented plane wave (LAPW) method, is renowned for its precision in calculating energy band structures. The LAPW method allows for a highly accurate representation of the electronic wave functions, making it one of the most reliable methods for investigating the electronic and optical properties of complex structures. By applying this method, we can achieve a detailed understanding of the material's behavior under various external influences, such as pressure and mechanical stress, thereby providing valuable insights for the development of advanced optoelectronic devices [19].

Using this advanced computational code, we simulate both crystal structures and nanostructures to predict a comprehensive array of optoelectronic properties. By solving the Kohn-Sham relations within the framework of a crystal lattice, we accurately determine the electronic and magnetic structures of the materials. This detailed approach allows us to gain profound insights into the material's behavior, facilitating the design and optimization of next-generation optoelectronic devices. The Kohn-Sham equations, derived from Density Functional Theory (DFT), provide a framework for describing the behavior of electrons in a many-body system. They achieve this by transforming the complex many-electron problem into a set of more manageable single-electron

problems, each moving in an effective potential that accounts for electron-electron interactions. This transformation simplifies the computational process while retaining the essential physics of the system.

The Generalized Gradient Approximation (GGA) further enhances the accuracy of these calculations by incorporating the gradients of the electron density. Unlike the Local Density Approximation (LDA), which considers the electron density to be locally uniform, the GGA accounts for the spatial variations in the density. This inclusion of density gradients allows for a more precise description of the exchange-correlation energy, leading to improved predictions of material properties. These approximations, by addressing the limitations of mean-field approaches, enable the resolution of complex issues in electronic structure calculations. The GGA's ability to provide a better approximation of the exchange-correlation functional makes it particularly valuable for studying systems with significant variations in electron density, thereby offering a more accurate and reliable depiction of the material's electronic behavior.

In this research, we examine the optical characteristics of two carbon nano-structures using caculational techniques enhanced by the Generalized Gradient Approximation (GGA). We utilize meshing grids of 1x12x12 and 1x25x25 for k-points within the first Brillouin zone. The Perdew-Burke-Ernzerhof (PBE) approach [20], is employed for these k-point computations, while the Monkhorst-Pack scheme is applied to address exchange-correlation interactions [21]. This methodology ensures a thorough and precise analysis of the optical aspects of the nano-structures. The Monkhorst-Pack approximation is a method used to sample the Brillouin zone in electronic property calculations, providing a systematic way to choose k-points for integration over the Brillouin zone, which is crucial for accurate electronic structure calculations [22]. The calculation input parameters are RMTKmax = 7, Gmax = 12 Ry$^{\wedge 1/2}$, lmax = 8. The Kramers-Kronig equations and the Random Phase Approximation (RPA) approach are utilized to derive various parts of the dielectric function [23]. The Kramers-Kronig relations are fundamental mathematical principles that link the imaginary and real components of a complex function. These relations ensure that the calculated dielectric function adheres to the principles of causality and physical consistency, providing a coherent description of the material's response to electromagnetic fields. The RPA describes the response of an electron gas to external perturbations, accounting for the collective motion of electrons and enhancing the accuracy of optical property predictions.

PENTA-GRAPHENE

In 2015, researchers predicted the existence of a novel two-dimensional carbon allotrope, termed penta-graphene, which was identified as an indirect bandgap semiconductor [11]. This groundbreaking discovery spurred extensive research into the optoelectronic properties of penta-graphene, focusing on its synthesis feasibility and potential applications in nanoelectronics. Subsequent studies have aimed to elucidate its electronic structure, optical behavior, and mechanical properties, thereby assessing its suitability for integration into advanced nano electronic devices.

In this study, we delve into the optical aspects of penta-graphene when subjected to buckling induced by stress. Utilizing fundamental calculations grounded on density functional theory, we aim to provide a comprehensive understanding of its behavior under these conditions. Our results indicate that this nanostructure, under the specified conditions, holds significant promise for the growth of versatile optoelectronic devices, potentially revolutionizing the field of nanoelectronics.

The two-dimensional penta-graphene, illustrated in Figure 1, is defined by space group no. 113 (P-421m) and exhibits a tetragonal lattice structure.

This lattice comprises two distinct carbon-carbon bond lengths, designated as C1 and C2. The C2 atomic layer, exhibiting sp3 hybridization, is situated between two layers of C1, which display sp2 hybridization. As illustrated in Figure 1, the lattice constants of the penta-graphene structure have been optimized using a thermodynamic model based on the Birch-Murnaghan equations [24].

$$E(V) = E_0 + \frac{9B_0V_0}{16}\left\{\left[\left(\frac{V_0}{V}\right)^{2/3} - 1\right]^3 B_0'\right\} + \frac{9B_0V_0}{16}\left\{\left[\left(\frac{V_0}{V}\right)^{2/3} - 1\right]^2 \left[6 - 4\left(\frac{V_0}{V}\right)^{2/3}\right]\right\} \quad (1)$$

In Equation (1), the optimal volume energy is calculated using the lattice parameters (a) and (b). Here, B_0' denotes the bulk modulus under applied pressure, B_0 represents the bulk modulus at zero pressure, and (V_0) is the initial volume. Figure 1(a) provides top and side views of the penta-graphene two-dimensional crystal supercell, while Figure 1(b) shows the volume versus energy curve for penta-graphene. The least point on the curve in Figure 1(b) corresponds to the ground state volume, indicating the lowest energy state of the

unit cell. This optimal volume energy is crucial for understanding the material's stability and mechanical properties under different conditions. Based on the equilibrium volume obtained, the optimized lattice parameters are (a = b = 3.649 A°), and the width between the lower and upper layers of the C1 atoms, referred to as the buckling (δ), is (0.589 A°). As a result, the total width of the two-dimensional penta-graphene is (1.178 A°).

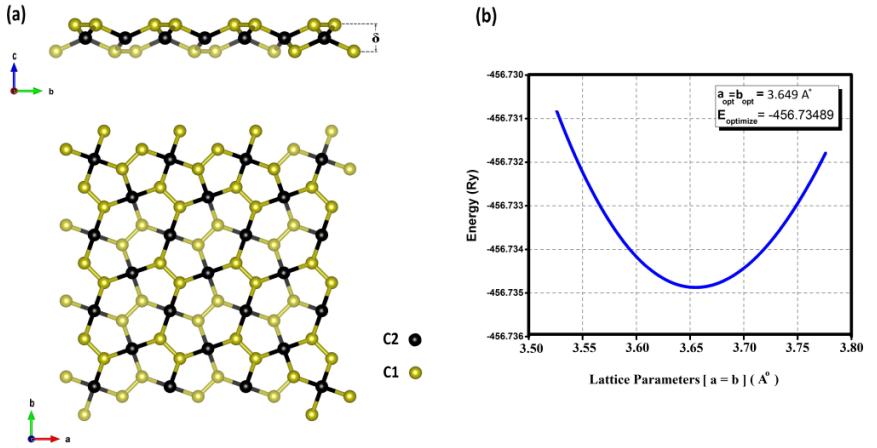

Fig.1. **(a)** Top and side views of the Penta-graphene supercell, **(b)** Energy vs lattice parameters unit cell of Penta-graphene

Table 1 presents the ground state structural parameters of penta-graphene, obtained using the PBE-GGA approach. These values are compared with earlier reported data from other computational approaches [12].

Table 1: Optimized structural data of Penta-graphene

Method	Optimized lattice (A^0)	Buckling (A^0)	Bond length (A^0)	E_{opt} (Ry)
PBE-GGA (This work)	a = b = 3.649	δ = 0.589	C1-C2 = 1.543 C1-C1 = 1.342	-456.735
LDA	a = b = 3.67	δ = 0.597	C1-C2 = 1.58 C1-C1 = 1.37	-455.234
GGA	a = b = 3.60	δ = 0.545	C1-C2 = 1.51 C1-C1 = 1.31	-458.444

Figure 2 illustrates the band structure and the total density of states (DOS) in its ground state. The analysis reveals that penta-graphene is an indirect band gap semiconductor with 2.231 eV band gap. The valence band maximum (VBM) is located along the Γ–X, while the conduction band minimum (CBM) is situated along the M–Γ. These findings are consistent with previously stated values in the literature [12].

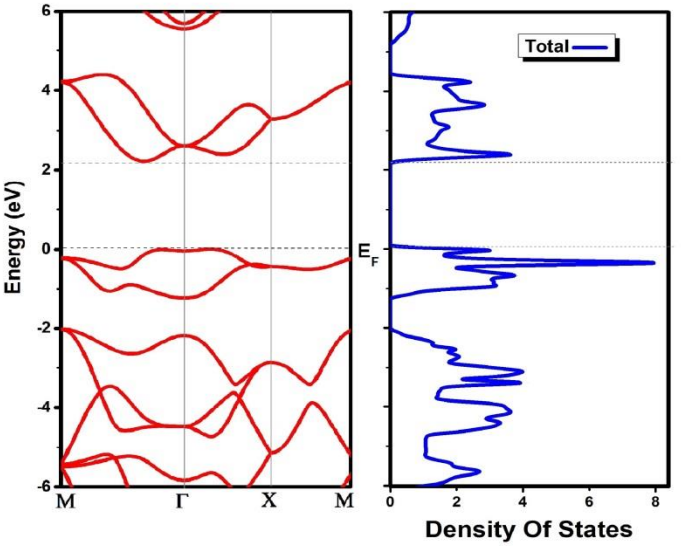

Fig.2. The band structure and electronic density of states (DOS) of penta-graphene

Figure 3 provides valuable insights: the bandgap and total energy were analyzed while reducing buckling by up to 12%. Notably, as the buckling constant decreases, both the total energy and system stability exhibit a slight decline, as indicated by the blue curve in **Figure 3**. This decline suggests that the structural integrity of penta-graphene is somewhat sensitive to buckling variations.

Furthermore, the bandgap shifts due to variations in buckling, illustrated by the violet curve in Figure 3. Specifically, imposing vertical stress reduces the bandgap of penta-graphene. This reduction in bandgap under vertical stress implies that the electronic aspects of penta-graphene can be adjusted by

mechanical deformation, which could be advantageous for various applications in nanoelectronics and flexible devices. The ability to modulate the bandgap through mechanical means adds a layer of versatility to the material, potentially enhancing its applicability in future technological advancements.

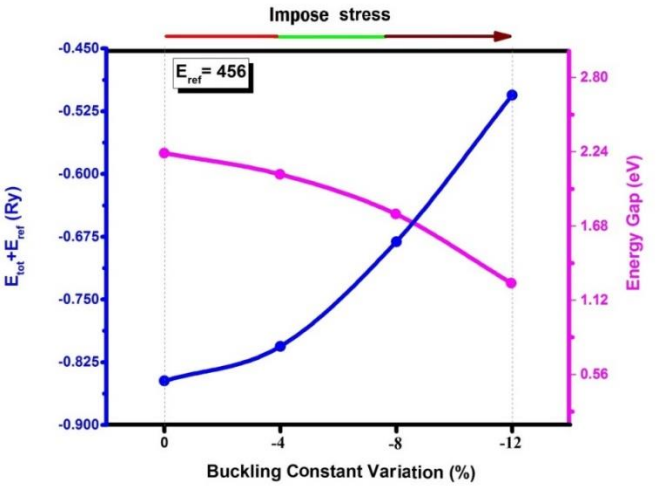

Fig.3. Band gap and total energy variation of penta-graphene under the buckling effects

A. Penta-graphene optical properties

In this section, we examine several significant optical aspects of penta-graphene, including the joint density of states (DOS), the imaginary and real components of the dielectric function, energy loss, reflectivity, and absorption. These properties are analyzed for penta-graphene in its ground state and under buckling variations of up to 12%. To induce variations in buckling, vertical stress is applied to the nanosheet, and the optical aspects are investigated and planned in the Z direction.

The joint density of states (joint DOS) is analyzed to investigate the optical inter-band transitions from occupied to unoccupied states, as depicted in Figure 4. This figure shows the optical joint DOS in the Z polarization, under stress conditions with 0%, 4%, 8%, and 12% buckling reduction. The joint DOS provides insight into the number of available electronic states that can participate in optical transitions at a given energy level.

Figure 4 reveals that the joint DOS spectrum diminishes as stress is applied to the nanomaterial. This reduction indicates that the application of stress affects the electronic structure of penta-graphene, leading to fewer available states for optical transitions. Such changes in the joint DOS under stress conditions are crucial for understanding how mechanical deformation influences the optical properties of the material. These insights are essential for the design and optimization of optoelectronic devices, where the material may be subjected to various stress conditions during operation. As indicated in Figure 4, a rise in stress consequences in a reduction of the buckling parameter in the Z direction." Consequently, the sharp peak at approximately 11 eV in the ground state shifts towards 14 eV and decreases in slope when stress is applied up to 12%.

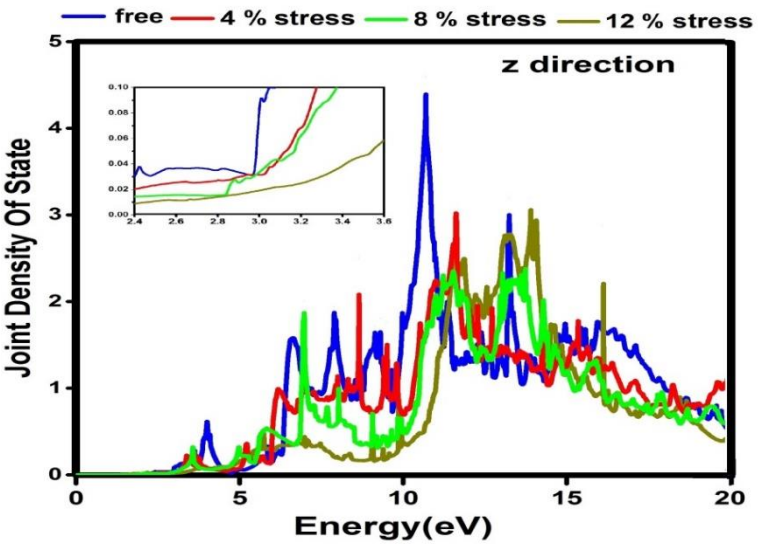

Fig.4. Joint Density of States (DOS) of the penta-graphene under stress condition

The complex dielectric function, which comprises both imaginary and real part, serves as a crucial factor in understanding various optical properties, including absorption and reflectivity spectra. This function is described by the following equation [25-28]:

$$\boldsymbol{\varepsilon_{complex}} = \mathfrak{R} + \mathbf{i}\,\mathfrak{I}\boldsymbol{\varepsilon} \quad (2)$$

The real component, derived by the Kramers-Kronig relations, is essential for understanding the optical properties of materials. This component provides insights into the dispersion and phase velocity of electromagnetic waves as they propagate through the material. The real part is given by the following equation:

$$\mathfrak{R}\varepsilon^{\alpha\beta}(\omega) = \delta_{\alpha\beta} + \frac{2}{\pi} Pr. \int_0^{\infty} \frac{\mathfrak{I}\,\varepsilon^{\alpha\beta}(\omega\prime)}{\omega\prime^2 - \omega^2}\, \omega' d\omega' \quad (3)$$

Here, ($Pr.$) denotes the Cauchy principal value. Additionally, the effective factor in the inter-band optical transitions between unoccupied (*fk*) and occupied (*ik*) states is represented by the imaginary component. This can be expressed by the following equation [29-30]:

$$\mathfrak{I}\varepsilon^{\alpha\beta}(\omega) = \frac{4\pi e^2}{m^2\omega^2} \sum_{i,j} \int \frac{2d^3k}{(2\pi)^3} |\langle ik|P_\alpha|fk\rangle|^2 f_i^k (1 - f_f^k) \delta(E_f^k - E_i^k - \bar{h}\omega) \quad (4)$$

The imaginary and real components of penta-graphene under stress conditions of 0%, 4%, 8%, and 12% buckling reduction are illustrated in Figures 5 and 6. Figure 5 indicates a sharp transition peak at approximately 6 eV in the unstressed state, which diminishes as stress increases up to 12%. Additionally, new sharp peaks appear for modes affected by buckling at stress levels of 8% and 12%, emerging at progressively higher energy levels within the 10 to 12 eV range.

Similarly, Figure 6 depicts the imaginary component. When stress is applied, the peak transition energy around 10 eV decreases. However, a resurgence of transition peaks is observed at stress levels of 8% and 12%, occurring at energies around 13 to 14 eV. These results propose a correlation between the optical and electronic behaviors of penta-graphene under varying stress conditions.

The alignment of these optical aspects with the electronic behavior under stress situations suggests that penta-graphene's dielectric function is highly sensitive to mechanical deformation. This sensitivity could be leveraged to tailor the

material's optical properties for specific applications, such as in optoelectronic devices where precise control over absorption and reflectivity is crucial.

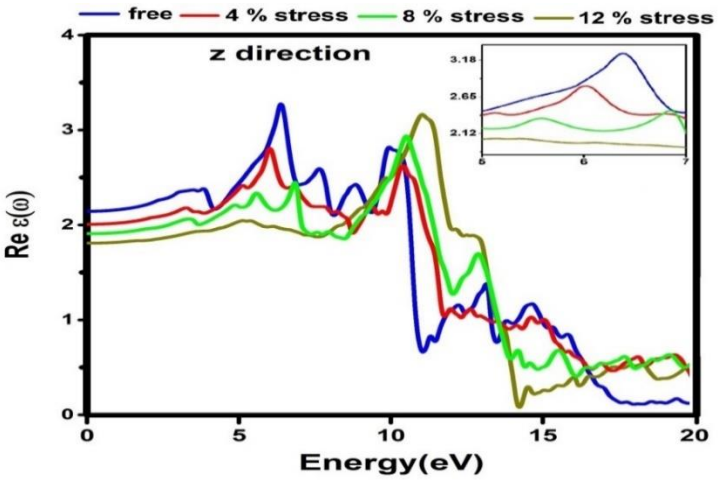

Fig.5. Real part plot of the dielectric function of the penta-graphene under stress

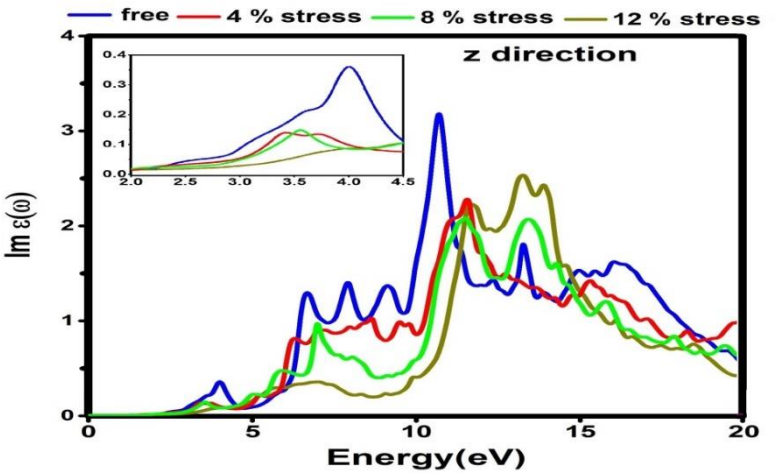

Fig.6. Imaginary part of the dielectric function of the penta-graphene under stress

Two critical aspects in the analysis of optical aspects are absorption and reflectivity. Figures 7 and 8 show the absorption and reflectivity spectra of the 2D penta-graphene nanostructure, respectively. These spectra are significantly affected by variations in buckling, which are induced by applying 0%, 4%, 8%, and 12% stresses.

Based on the figures, the absorption and reflectivity spectra from visible light energy up to approximately 11 eV exhibit a decreasing trend as stress increases up to 12%. This pattern persists for the 4% stress state at upper optical energies, extending up to 20 eV. However, within the energy range of 13 to 15 eV, for stress levels of 8% and 12%, there is a notable surge in the absorption and reflectivity amplitudes, with pronounced peaks emerging around 14 eV."

These variations in optical performance under varying stress situations are closely linked to the electronic properties of penta-graphene. Specifically, the modification from an indirect bandgap to a direct bandgap semiconductor, along with a reduction in the bandgap, contributes to these observed optical phenomena. The ability to modulate the absorption and reflectivity through mechanical stress highlights the potential of penta-graphene for applications in optoelectronic devices, where precise control over optical properties is essential.

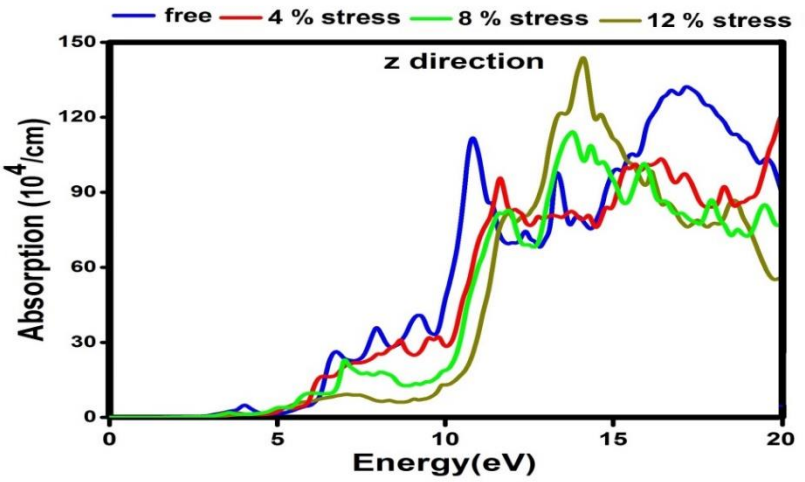

Fig.7. Absorption of the penta-graphene under buckling stresses

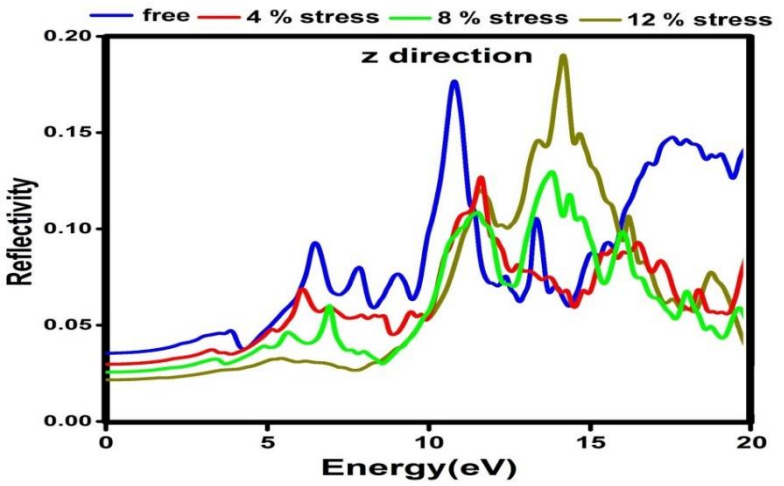

Fig.8. Reflectivity spectrum of the penta-graphene under buckling stresses

T-CARBONE

T-Carbon, a three-dimensional cubic carbon nano-allotrope, has a relatively minor density and belongs to the Fd3m space group, akin to diamond. As shown in Figure 9(a), this structure is formed by substituting each atom in the diamond lattice with a carbon tetrahedron. The orientations of these tetrahedra in the [100], [110], and [111] directions are depicted in Figures 9(b-d), respectively [14].

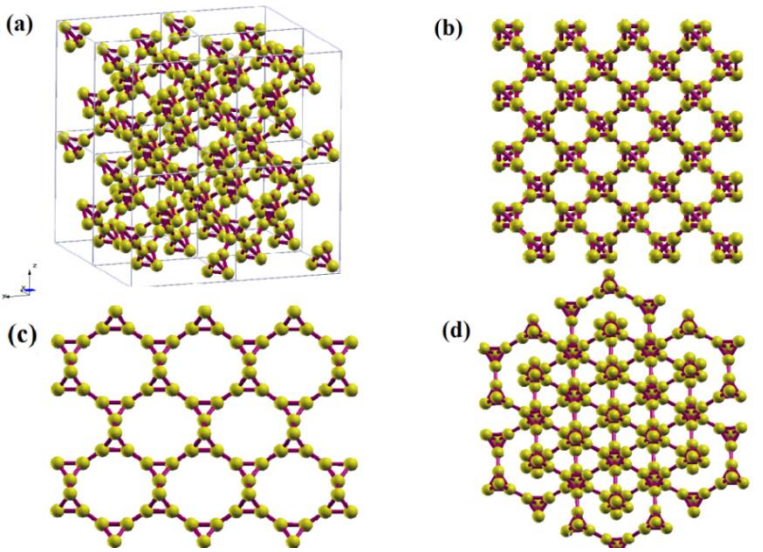

Fig.9. **(a)** cubic crystalline structure of T-carbon **(b)–(d)** Views from [100], [110], and [111] directions of T-carbon

Table 2 presents the structural aspects of T-Carbon, including the ground state lattice parameter, cohesive energy, band gap, and total energy obtained by the PBE-GGA approach [14]. These values are equated with earlier reported results from other computational approaches [7]. The comparison highlights the consistency and accuracy of the PBE-GGA method in predicting the structural characteristics of T-Carbon, providing a comprehensive understanding of its properties.

Table 2: Structural data, lattice parameter, band gap and cohesive energy for T-Carbon

Method	$l(A^0)$	$E_G(eV)$	$E_{cho}(eV/atom)$
LDA	**7.446**	**2.22**	**7.577**
GGA	**7.52**	**2.25**	**6.573**
PBE-GGA (this work)	**7.52**	**2.257**	**6.545**

Figure 10 presents the energy band structure and density of states (DOS) of T-Carbon in its ground state. The analysis indicates that 3D T-Carbon is a direct band gap semiconductor with a band gap of 2.257 eV. Both the valence band maximum (VBM) and the conduction band minimum (CBM) are situated at the Γ point. These findings align well with previously reported values [7], validating the accuracy of the current computational approach.

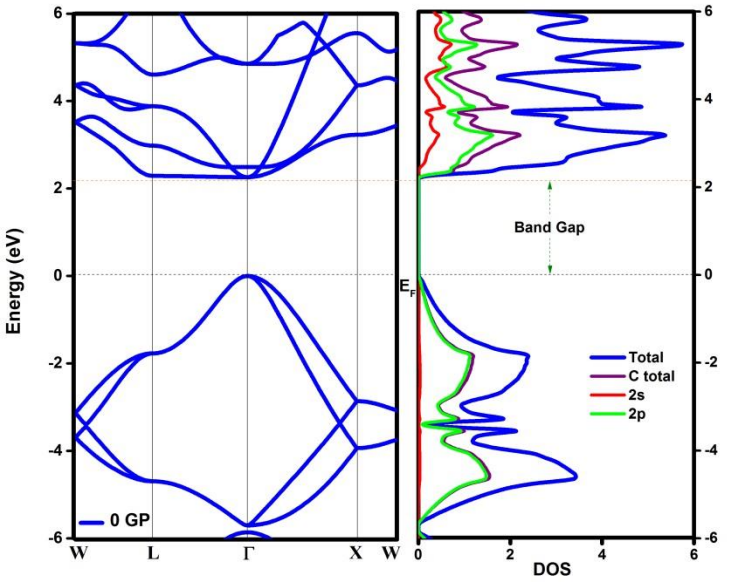

Fig.10. The band structure and electronic density of states (DOS) of T-Carbon

Figure 11 presents the calculated energy band gap and total energy disparity of T-Carbon under pressures up to 9 GPa. The results indicate that as this nano-allotrope is subjected to increasing hydrostatic pressure, the system's stability decreases, as depicted by the blue curve. This decline in stability is limited but noticeable up to the maximum applied pressure of 9 GPa. Concurrently, the band gap of T-Carbon decreases under the influence of hydrostatic pressure, as shown by the red curve in Figure 11. These findings suggest that hydrostatic pressure significantly impacts both the structural stability and electronic properties of T-Carbon, potentially altering its suitability for various applications.

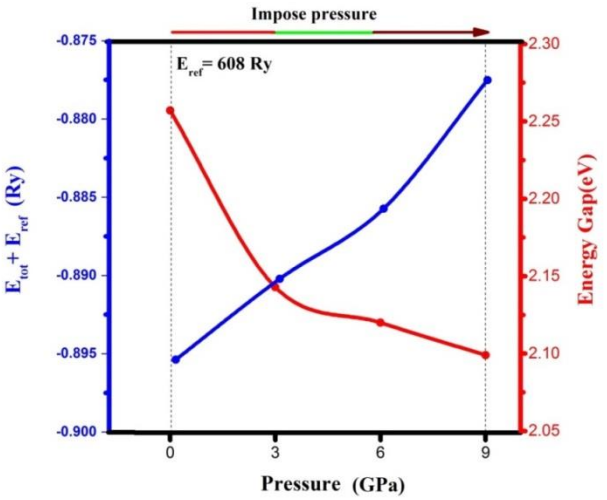

Fig.11.Band gap and total energy of T-Carbon under pressure

B. T-Carbon optical properties

To gain a deeper understanding of T-Carbon's performance under hydrostatic pressure, we examine several key optical properties within the energy range of 0-20 eV. This analysis focuses on the optical transitions from occupied to unoccupied states by evaluating the joint density of states. The study considers both the optimal state and conditions under applied pressures up to 9 GPa.

Figure 12 presents the joint density of states spectrum for T-Carbon under these conditions. The figure reveals that as pressure increases up to 9 GPa, there is a slight decrease in the joint DOS spectrum. This reduction indicates that the application of pressure affects the electronic transitions within the material, potentially altering its optical properties. Understanding these changes is crucial for optimizing T-Carbon's performance in various applications, particularly those involving high-pressure environments.

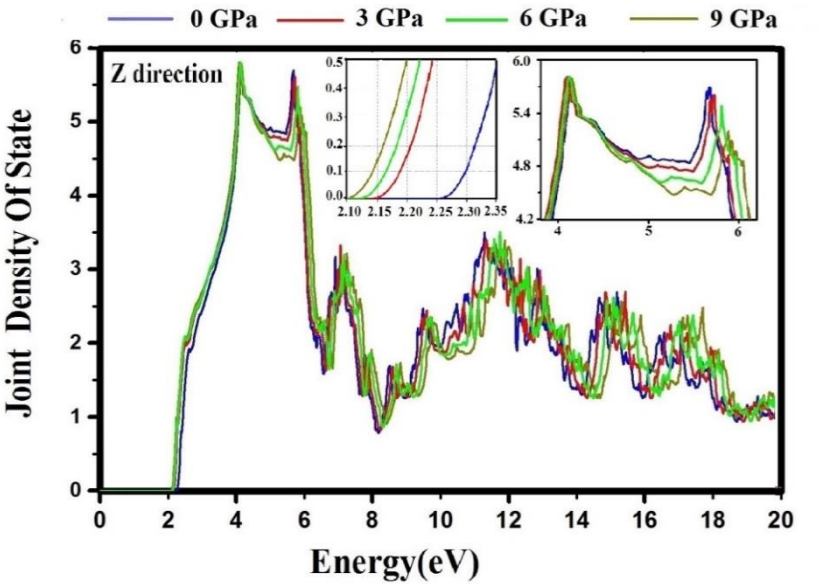

Fig.12. Joint Density of States (DOS) of the T-Carbon under pressure condition

Figures 13 and 14 illustrate the real and imaginary spectra of the dielectric function under pressures up to 9 GPa in the Z direction. The spectra indicate a slight increase in the real component as pressure rises to 9 GPa, while the imaginary component exhibits a modest decrease under the same conditions. Overall, the application of pressure induces minor variations in both components of the complex dielectric function for this nanostructure.

These observations suggest that T-Carbon's optical properties are somewhat sensitive to hydrostatic pressure, although the changes are relatively modest. Understanding these variations is essential for potential applications where T-Carbon might be subjected to different pressure conditions, as even slight modifications in the dielectric function can impact the material's performance in optoelectronic devices.

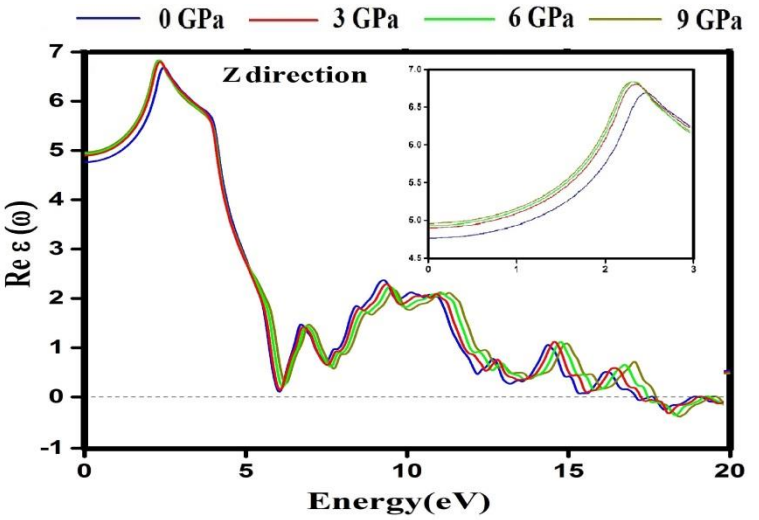

Fig.13. Real part plot of the dielectric function of T-Carbon under pressure

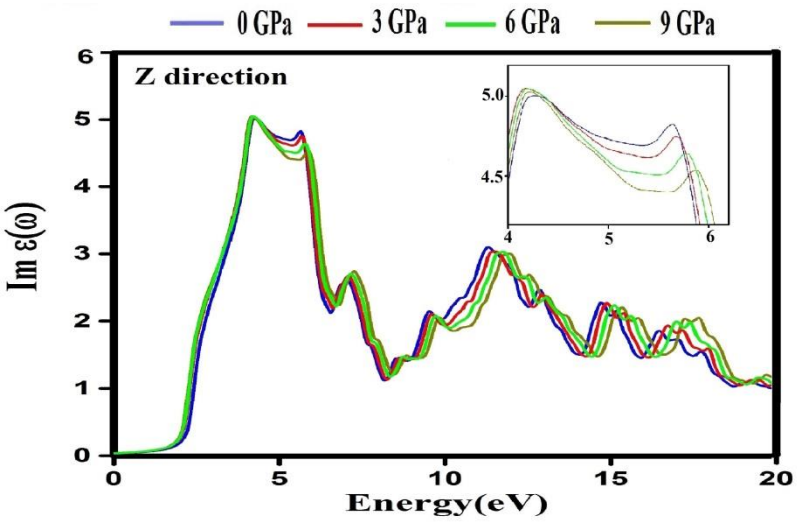

Fig.14. Imaginary part plot of the dielectric function of T-Carbon under pressure

Two critical features for investigating optical properties are absorption and reflectivity. Here, the optical aspects of the T-Carbon crystal under pressures up to 9 GPa have been analyzed. These spectra are illustrated in the Z direction in Figures 15 and 16. As shown in these figures, the pressure on the crystal increases up to 9 GPa, there is a gradual increase in both the absorption and reflectivity spectra. This suggests that the application of pressure enhances the optical response of T-Carbon, potentially making it more effective for applications that require precise control over optical absorption and reflectivity.

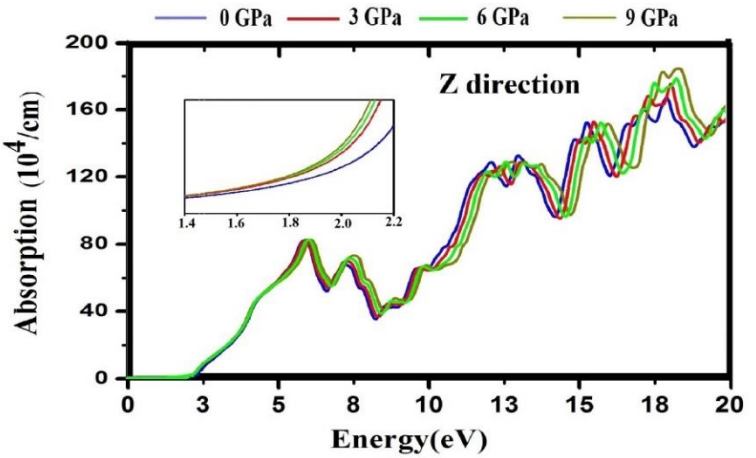

Fig.15. Absorption of T-Carbon crystal under pressure

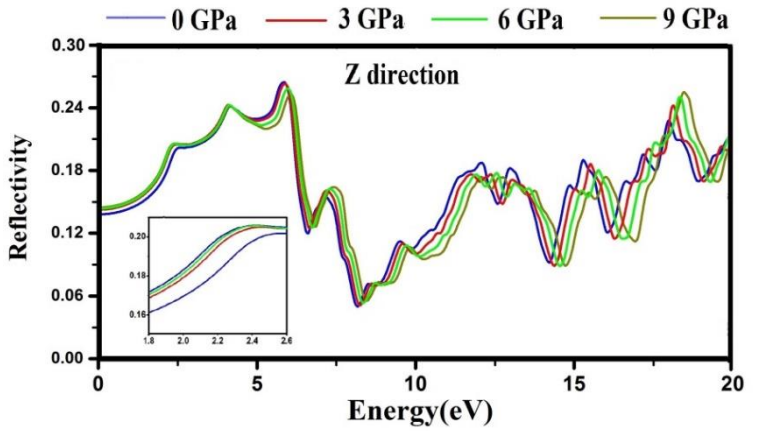

Fig.16. Reflectivity spectrum of T-Carbon crystal under hydrostatic pressures

Finally, the energy loss (ELOSS) spectrum of the T-Carbon is examined under the specific situations applied in this study, as depicted in the Z direction in Figure 17. The figure illustrates a gradual change in the ELOSS spectrum of this nano-allotrope when subjected to pressure up to 9 GPa. This observation is significant as it highlights the sensitivity of the T-Carbon crystal's energy loss characteristics to external pressure. Notably, the plasma frequency in the T-Carbon is observed between 23 and 24 eV. As shown in the figure, this frequency rate gradually shifts to upper values as the pressure increases towards 9 GPa, indicating a direct correlation between pressure and plasma frequency.

These observations suggest that the application of hydrostatic pressure influences the energy loss characteristics of T-Carbon, potentially affecting its performance in applications where energy dissipation is a critical factor. Understanding these shifts in plasma frequency under varying pressure conditions is essential for optimizing the material's properties for specific technological applications.

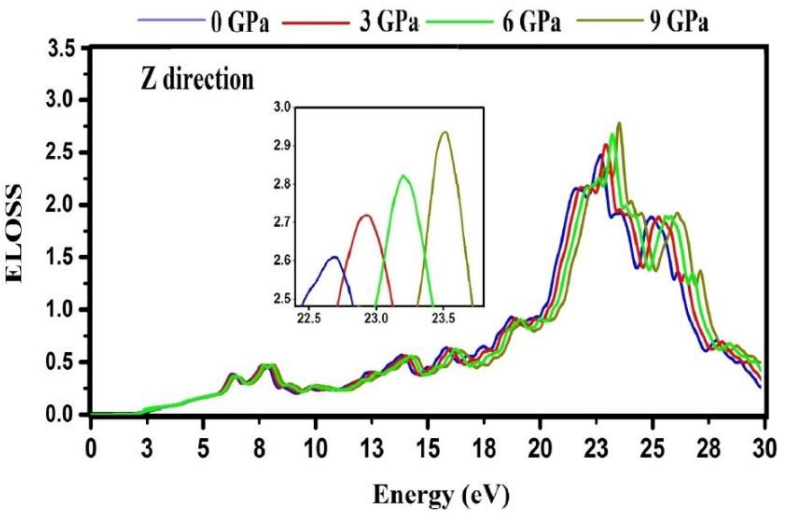

Fig.17. Energy loss of T-Carbon under pressure

CONCLUSION

In this pioneering study, we investigated the optical properties of two novel carbon nano allotropes: Penta-graphene and T-Carbon. Utilizing first-principles calculations within the DFT, we explored their intricate behaviors. Our findings illuminate the optical landscape of these nanostructures. T-Carbon, a 3D nanostructure, exhibits subtle fluctuations in its optical properties under applied pressure, which align with its electronic behavior and underscore its potential in optoelectronic applications. Specifically, the optical properties of T-Carbon show gradual changes in response to hydrostatic pressure, reflecting its stability and adaptability in various conditions. Meanwhile, Penta-graphene, a 2D nanostructure, demonstrates reductions in its optical spectra under stress up to 4%, with significant shifts observed beyond this threshold. These optical characteristics closely mirror its electronic properties, indicating a harmonious interplay between mechanical stress and electronic behavior. This sensitivity to stress suggests that Penta-graphene could be effectively utilized in flexible and responsive optoelectronic devices. Both Penta-graphene and T-Carbon exhibit unique optical signatures and demonstrate compatibility under specific conditions, making them promising candidates for innovative optoelectronic devices. Their distinct optical and electronic properties, coupled with their responsiveness to external stimuli, highlight their potential as foundational materials in the development of next-generation technologies.

ACKNOWLEDGMENT

This study is supported by, Khatam Al-Anbia University, Tehran, Iran. Hamidreza Alborznia would like to thank Fateme Afrashte, and Alireza Alborznia for their interest in this work**.**

REFERENCES

[1] C.N.R. Rao, H.S.S. Ramakrishna Matte, U. Maitra, *Graphene Analogues of Inorganic Layered Materials, Angewandte Chemie International Edition, 52 (2013) 13162-13185. F. Diederich, M. Kivala, All-Carbon Scaffolds by* Rational Design, Adv. Material, 22 (2010) 803. https://doi.org/10.1002/anie.201301548

[2] A. Hirsch, *The era of carbon allotropes*, Nature Materials, 9 (2010) 868. https://doi.org/10.1038/nmat2885

[3] Q. Li, Y. Ma, A.R. Oganov, H. Wang, H. Wang, Y. Xu, T. Cui, H.-K. Mao, G. Zou, *Superhard Monoclinic Polymorph of Carbon*, Physical Review Letters, 102 (2009) 175506. https://doi.org/10.1103/PhysRevLett.102.175506

[4] K. Umemoto, R.M. Wentzcovitch, S. Saito, T. Miyake, *Body-Centered Tetragonal C_4: A Viable sp^3 Carbon Allotrope*, Physical Review Letters, 104 (2010) 125504.

[5] J.-T. Wang, C. Chen, Y. Kawazoe, *Low-Temperature Phase Transformation from Graphite to sp^3 Orthorhombic Carbon*, Physical Review Letters, 106 (2011) 075501.

https://doi.org/10.1103/PhysRevLett.106.075501

[6] M. Nayeri, P. Keshavarzian, M. Nayeri, *A Novel Design of Penternary Inverter Gate Based on Carbon Nano Tube*, Journal of Optoelectronic Nano Structures, 3 (2018) 15-26.

https://dorl.net/dor/20.1001.1.24237361.2018.3.1.2.3

[7] X.-L. Sheng, Q.-B. Yan, F. Ye, Q.-R. Zheng, G. Su, *T-Carbon: A Novel Carbon Allotrope*, Physical Review Letters, 106 (2011) 155703. http://dx.doi.org/10.1103/PhysRevLett.106.155703

[8] D. Li, K. Bao, F. Tian, Z. Zeng, Z. He, B. Liu, T. Cui, *Lowest enthalpy polymorph of cold-compressed graphite phase*, *Physical Chemistry Chemical Physics*, 14 (2012) 4347-4350.

https://doi.org/10.1039/C2CP24066A

[9] C. He, L. Sun, C. Zhang, X. Peng, K. Zhang, J. Zhong, *Four superhard carbon allotropes: a first-principles study*, Physical Chemistry Chemical Physics, 14 (2012) 8410-8414.

https://doi.org/10.1039/C2CP40531H

[10] H. Alborznia, *First-principle study of the strain compressive strain induced on optoelectronic aspects of 2-dimensional B2C nanostructure*, Surface Review and Letters, 29 (2022) 2250078.

https://doi.org/10.1142/S0218625X22500780

[11] Zhang, S.; Zhou, J.; Wang, Q.; Chen, X.; Kawazoe, Y.; Jena, P. *Penta-Graphene: A New Carbon Allotrope*. Proc. Natl. Acad. Sci., 112 (2015) 2372. https://doi.org/10.1073/pnas.1416591112

[12] H. Alborznia, M. Naseri, N. Fatahi, *Buckling strain effects on electronic and optical aspects of penta-graphene nanostructure,* Superlattices and Microstructures,133(2019) 106217.

https://doi.org/10.1016/j.spmi.2019.106217

[13] M. Roohollahi, M. R. Shayesteh, M. Pourahmadi, *Improved Perovskite Solar Cell Performance Using Semitransparent CNT Layer*. Journal of Optoelectronic Nano Structures, 8 (2023) 32-46.

https://doi.org/10.30495/jopn.2023.29770.1253

[14] H. Alborznia, M. Naseri, N. Fatahi, *Pressure effects on the optical and electronic aspects of T-Carbon: A first principles calculation,* Optik, 180 (2019) 125-133. https://doi.org/10.1016/j.ijleo.2018.11.077

[15] D.M. Hoat, Sh. Amirian, H. Alborznia, A. Laref, A.H. Reshak, M. Naseri, *strain effect on the electronic and optical properties of 2D Tetrahexcarbon: a DFT-based study*, Indian Journal of physics, 95 (2021) 2365. https://doi.org/10.1007/s12648-020-01913-1

[16] H. Alborznia, *DFT- based study of the strain variation effects on optical and electronic aspects of TH-carbon monolayer*, International Journal of Modern Physics B, 38 (2024) 2450085.

https://doi.org/10.1142/S0217979224500851

[17] H. Alborznia, S.T. Mohammadi, *Biaxial stress and strain effects on optical and electronic aspects of B2C nanostructure: a first-principles calculation,* Indian Journal of physics, 32 (2022).

https://doi.org/10.1007/s12648-021-02272-1

[18] P. Giannozzi et al., *J. Phys. Condens. Matter 21, 395502(2009); computer code QUANTUM-ESPRESSO,* http://www.quantum-espresso.org

[19] *P. Blaha, K. Schwarz, G.K.H. Madsen, D. Kvasnicka, J. Luitz,K. Schwarz, An augmented PlaneWave+Local Orbitals Program for calculating crystal properties revised edition* WIEN2k 13.1 (release 06/26/2013) Wien2K users guide, ISBN 3-9501031-1-2.

[20] J.P. Perdew, K. Burke, M. Ernzerhof, *Generalized Gradient Approximation Made Simple*, Phys. Rev. Lett. 77 (1996) 3865-386. https://link.aps.org/doi/10.1103/PhysRevLett.77.3865

[21] J. Heyd, G.E. Scuseria , M. Ernzerhof, *Hybrid functionals based on a screened Coulomb potential*, J. Chem. Phys. 118 (2003) 8207. https://doi.org/10.1063/1.1564060

[22] H.J. Monkhorst, J.D. Pack, *Special points for Brillouin-zone integrations*, Physical Review B, 13 (1976) 5188-5192.

https://link.aps.org/doi/10.1103/PhysRevB.13.5188

[23] H. Ehrenreich, M.H. Cohen, *Self-Consistent Field Approach to the Many-Electron Problem*, Phys. Rev. 115 (1959) 786-790.

https://link.aps.org/doi/10.1103/PhysRev.115.786

[24] F. Birch, *Equation of state and thermodynamic parameters of NaCl to 300 kbar in the high-temperature domain*, J. Geophys. Res. B 83 (1978) 1257-1268. https://doi.org/10.1029/JB091iB05p04949

[25] R. Abt, C. Ambrosch-Draxl, P. Knoll, *Optical response of high temperature superconductors by full potential LAPW band structure calculations*, Physica B: Condensed Matter, 194-196 (1994) 1451-145. http://www.sciencedirect.com/science/article/pii/0921452694912254

[26] S. Damizadeh, M. Nayeri, F. Kalantari Fotooh, S.fotoohi, *Electronic and Optical Properties of SnGe and SnC Nanoribbons: A First-Principles Study*, Journal of Optoelectronic Nano Structures, 5 (2020) 67-86.

https://dorl.net/dor/20.1001.1.24237361.2020.5.4.5.6

[27] S. Amirian, H. Alborznia, S. Yalameha, *First-principles study on the stability and optoelectronic properties of the novel C6O2 nanostructure,* Solid State Communications, 394 (2024) 115693.

https://doi.org/10.1016/j.ssc.2024.115693

[28] R. Yahyazadeh, Z. Hashempour. *Effect of Hydrostatic Pressure on Optical Absorption Coefficient of InGaN/GaN of Multiple Quantum Well Solar Cells*, Journal of Optoelectronic Nano Structures, 8 (2023) 81-107. https://doi.org/10.30495/jopn.2021.27941.1221

[29] H. Alborznia, S. Amirian, M. Nazirzadeh, *Buckling variation effects on optical and electronic properties of GeP2S nanostructure: a first-principles calculation*, Opt. Quant. Electron. 54 (2022) 608.

https://doi.org/10.1007/s11082-022-04055-2

[30] H. Salehi, F. A. Hoseini, *First-Principles Study of Structure, Electronic and Optical Properties of HgSe in Zinc Blende (B3) Phase*, Journal of Optoelectronic Nano Structures, 4 (2019) 69-82.

https://dorl.net/dor/20.1001.1.24237361.2019.4.2.6.6